A Subwavelength Perfect Absorbing Metamaterial Patch Array Coupled with a Molecular Resonance

Michael F. Finch and Brian A. Lail

Department of Electrical and Computer Engineering
Florida Institute of Technology, 150 West University Blvd., Melbourne, FL, 32901, USA
mfinch2009@my.fit.edu, blail@fit.edu

Abstract ─ A perfectly absorbing metamaterial (PAMM) coupled with vibrational modes has varied applications ranging from surface-enhanced vibrational spectroscopy to biological sensing. This endeavor considers a subwavelength PAMM sensor design and analysis using a commercially available finite element method (FEM) solver and analytically with temporal coupled mode theory (TCMT). A carbon double oxygen bond (C=O) at 52 THz or 1733 cm^{-1} that resides in poly(methyl methacrylate), PMMA, will be used as a stand-in analyte. Normal mode splitting that results from the resonant coupling between the PAMM and analyte's molecular resonance is investigated and analyzed.

Index Terms ─ Electromagnetic Induced Absorption (EIA), Electromagnetic Induced Transparency (EIT), metamaterial, perfect absorbing, PMMA, resonant coupling, superscattering.

I. INTRODUCTION

Metamaterial are engineered materials that are designed with periodic or aperiodic elements known as meta-atoms [1]. A perfect absorbing metamaterial (PAMM), as the name implies, is designed to "perfectly" absorb incident fields, and have been described with a metamaterial impedance matched to free space [2-5]. A commercially available finite element method solver, Ansys high frequency structural simulator (HFSS), is employed to design and simulate a gold patch array metasurface with ground plane to form a subwavelength optical resonant cavity.

Resonant coupling results in avoidance crossing dispersion relationships, or normal mode splitting, that is described with temporal coupled mode theory (TCMT) [2, 6-9]. Coupled resonant models have been used a classical analogy treatment of quantum phenomena, namely Fano resonance with bright/dark mode interactions [10-12], and electromagnetically induced transparency or absorption (EIT or EIA) [2, 13-17]. In a Fano resonance, EIT, or EIA treatment a molecular resonance is modeled as a dark mode. TCMT has also been used to describe light-matter interactions in polaritonic systems [18].

In the case of this work, poly(methyl methacrylate) (PMMA), a thermal plastic for very-large-scale integration (VLSI) and material for plastic fibers, has a carbon double oxygen (C=O) molecular resonance at 52 THz/1733 cm^{-1} with optical material properties measured using ellipsometry [19]. PMMA's C=O infrared (IR) active molecular bond will be used as an analyte stand-in to demonstrate the mode splitting. Metamaterial coupled to molecular resonances has varied applications including, but not limited to, biosensing and surface enhanced-vibrational spectroscopy [4, 9, 10, 13, 20, 21].

II. PAMM SENSOR

The PAMM unit cell under consideration is a gold patch stood-off above from a gold ground plane by a spacer of amorphous silicon as shown in Fig. 1. For the preliminary analysis of the PAMM, a thin overlay of material with the refractive index that of dispersionless PMMA is introduced to reduce the red shifting induced on the PAMM's resonance [4]. The PAMM spacer thickness range is on the order of 20 to 200 nm which results in a subwavelength nanoresonator cavity.

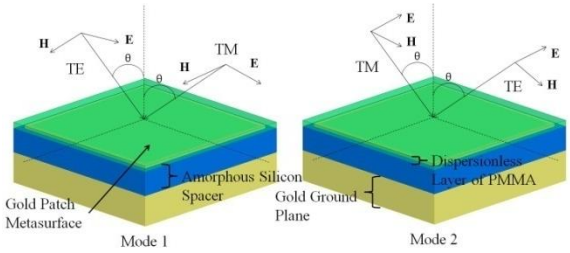

Fig. 1. PAMM unit cell modeled in Ansys HFSS.

A. Theory

Derived from circuit theory or mass spring relationships [2, 6, 21], it can be seen from the TCMT that the PAMM can be modeled as a single input uncoupled system (SI-US) as seen in Fig. 2. The TCMT

Submitted On: May 27, 2016
Accepted On: June 15, 2016

equations for normalized resonator energy "a" at resonator frequency ω_0 can be written as:

$$\frac{da}{dt} = j\omega_0 a - (\gamma_0 + \gamma_e)a + \alpha S^+, \quad (1.a)$$

$$S^- = cS^+ + da, \quad (1.b)$$

where [2, 6],

$$|\alpha| = \sqrt{2\gamma_e}, \quad (2.a)$$

$$d = \sqrt{2\gamma_e}, \quad (2.b)$$

$$c = -|\frac{\alpha}{d}| = -1, \quad (2.c)$$

and γ_0 and γ_e represent internal and external losses, respectively. The internal loss can be thought of as Ohmic loss within the PAMM or circuit resonator. External loss results from excitation that does not couple into the PAMM or resonator, but reflects or scatters out of the structure. The excitation and reflected field is denoted as S^+ and S^- respectively.

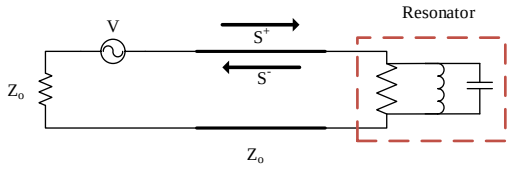

Fig. 2. Circuit visualization for a SI-US where the resonator circuit models the PAMM.

Given the single input description of the PAMM and from (1) and (2) it can be seen that the only scattering parameter is the reflection coefficient:

$$S^- = \left[\frac{j(\gamma_e-\gamma_0)+(\omega-\omega_0)}{j(\gamma_e+\gamma_0)-(\omega-\omega_0)}\right] S^+, \quad (3)$$

and at resonance (3) becomes:

$$S_{11}(\omega_0) = \frac{\gamma_e-\gamma_0}{\gamma_e+\gamma_0}. \quad (4)$$

Due to the ground plane in the PAMM the transmission spectrum can be taken as negligible; therefore,

$$A(\omega) = 1 - |S_{11}(\omega)|^2, \quad (5)$$

where A(ω) is the absorbed power in the PAMM. It can be seen from (4) when $\gamma_e = \gamma_0$ then $|S_{11}(\omega_0)|$ tends to zero, or A(ω) becomes unity. The condition $\gamma e = \gamma_0$ can be described via impedance matching and results in the "perfect absorption" condition in the metamaterial known as criticallycoupled [2, 3, 6]. The condition $\gamma_e < \gamma_0$ and $\gamma_e > \gamma_0$ is referred to as undercoupled and overcoupled respectively. The "coupling" in critically-(CC), under-(UC), and overcoupled (OC) is in reference to the impinging field "coupling" into the PAMM and not related to the molecular resonance.

B. PAMM numerical results

While maintaining the PAMM at approximately at 52 THz (molecular resonant frequency), the thickness of the A-Si spacers was varied. A case of OC, CC, and UC can be seen in Fig. 3 for spacer thickness of 150, 90, and 50 nm respectively. From (4), it can be seen that the CC case is the only case where approximately the perfect absorption condition is met. Figure 4 is the spectral and angular resolution for the absorption for the CC case for both incident modes seen in Fig. 1. It can be seen that the design patch metamaterial provides a polarization insensitive to transverse electrical (TE), transverse magnetic (TM), or either mode orientation while providing a wide-field-of-view [3]. With the use of the TCMT equations, the damping rates, external (γ_e) and internal (γ_0), were determined by a parametric fit and the absorption is plotted in Fig. 3 as seen as asterisks (*), and linear fit as seen in Fig. 5.

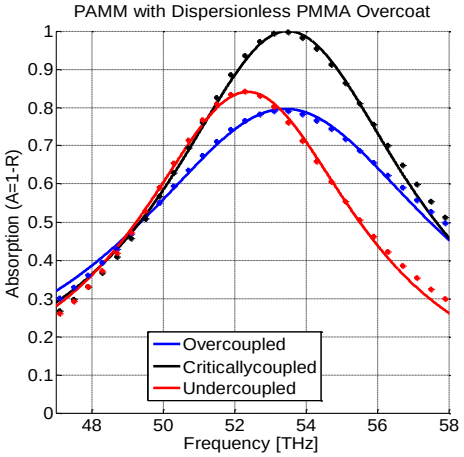

Fig. 3. Numerical (*) and mathematical model (solid line) results are shown for case of over-(OC), critically-(CC), and undercoupled (UC) cases.

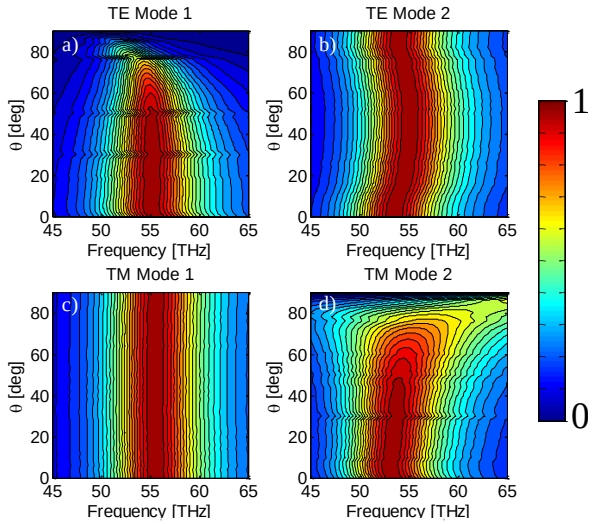

Fig. 4. Absorption spectra and angular-resolved for the criticallycoupled cases as seen in Fig. 1. Both TE (a, b) and TM (c, d) polarizations are shown for both mode orientations.

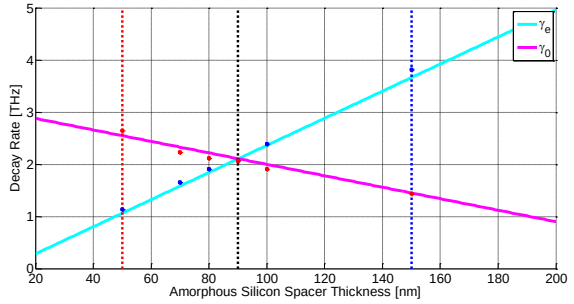

Fig. 5. Linear relationship between external (γ_e) and internal (γ_0) loss as a function of amorphous space thickness. CC case is seen at around 90 nm Si spacer thickness.

III. PAMM-MOLECULAR COUPLING

A. TCMT description

Similar to a EIT/EIA or Fano resonate description, the molecular resonance is a weak coupling to the incident field and is a spectrally narrow resonance, therefore; it can be model as a dark resonance mode [2, 10, 12, 13] as seen in the circuit realization in Fig. 6. However, the PAMM provides a spectrally broad resonance and couples very strongly with the incident field, and thus can be thought as a bright mode as seen in Fig. 6.

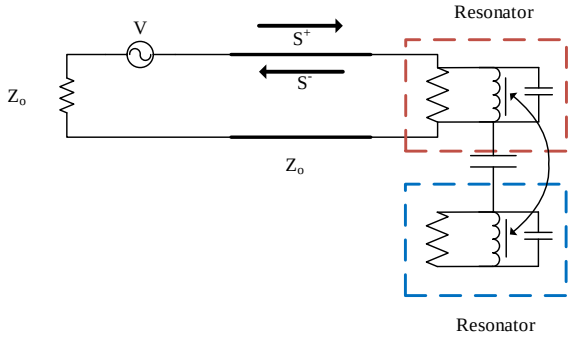

Fig. 6. Circuit visualization for a single input couple resonator system.

Using TCMT, an addition equation describing the molecule resonance, "a_2", with complex frequency $\omega_2 + j\gamma_2$. The interaction or mode coupling between the PAMM and molecule resonance is describe with the coupling strength "V". The coupling strength is a result of the interactions of the near field from the PAMM on to the PMMA molecular bond. The TCMT system of equations that results are as follow [2, 18]:

$$\frac{da_1}{dt} = j\omega_1 a_1 - (\gamma_1 + \gamma_e)a_1 + jVa_2 + \alpha {S_1}^+, \quad (6.a)$$

$$\frac{da_2}{dt} = j\omega_2 a_2 - \gamma_2 a_2 + jVa_1, \quad (6.b)$$

$$S^- = cS^+ + da_1. \quad (6.c)$$

B. PAMM molecular resonance coupled numerical results

With the introduction of the PMMA phonon resonance, it can be observed that for the CC and UC cases in mode splitting or EIT [12, 14] while OC case results in superscattering or EIA [15, 16] as seen in Figs. 7 and 8. Figure 8 (b) shows the avoidance crossing dispersion relation [8] where the variation of the only the A-Si spacer thickness resulting changing the PAMM resonances or absorption maximum spectrally.

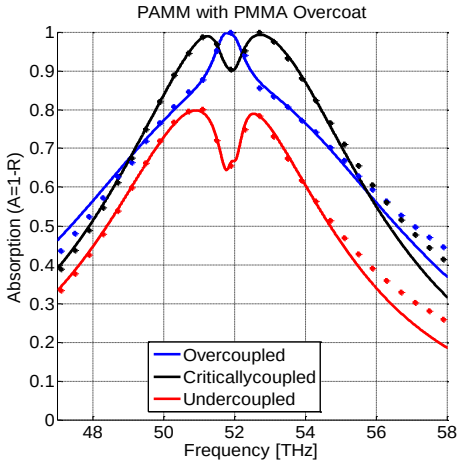

Fig. 7. Numerical (*) and mathematical model (solid line) results are shown for resonant coupling between PAMM and molecular resonance.

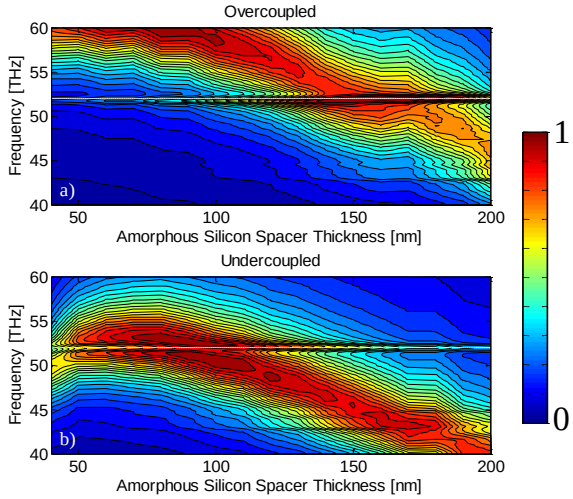

Fig. 8. Absorption spectra for PAMM resonantly coupled to a molecular resonance at 52 THz (white dashed line) for OC (a) and UC (b) cases for varies A-Si spacer thickness.

IV. CONCLUSION

With the use of finite element method and TCMT, a perfect absorbing patch metamaterial resonant coupled

to a C=O doubled bond at 52 THz of PMMA was investigated. EIT and EIA responses and anti-crossing dispersion are evident when resonated couple between a PAMM and molecule resonance is presented.

REFERENCES

[1] A. V. K., A. Boltasseva, and V. M. Shalaev, "Planar photonics with metasurfaces," *Science*, vol. 339, no. 6125, pp. 1232009-1-1232009-6, 2013.

[2] R. Adato, A. Artar, S. Erramilli, and H. Altug, "Engineered absorption enhancement and induced transparency in coupled molecular and plasmonic resonator systems," *Nano Letters*, vol. 13, no. 6, pp. 2584-2591, May 2013.

[3] C. Wu, B. Neuner, and G. Shvets, "Large-area, wide-angle, spectrally selective plasmonic absorber," *Physical Review B*, vol. 84, no. 7, pp. 075105:1-7, August 2011.

[4] K. Chen, R. Adato, and H. Altug, "Dual-band perfect absorber for multispectral plasmon-enhanced infrared spectroscopy," *ACS Nano*, vol. 6, no. 9, pp. 7998-8006, August 2012.

[5] N. I. Landy, S. Sajuyigbe, J. J. Mock, D. R. Smith, and W. J. Padilla, "Perfect metamaterial absorber," *Physical Review Letters*, vol. 100, no. 20, pp. 207402-207408, May 2008.

[6] H. A. Haus, *Waves and Fields in Optoelectronics*. Englewood Cliffs, NJ: Prentice-Hall, Inc., 1984.

[7] H. A. Haus and W. Huang, "Coupled-mode theory," *Proceeding of the IEEE*, vol. 79, no. 10, pp. 1505-1518, 1991.

[8] L. Novotny, "Strong coupling, energy splitting, and level crossings: A classical perspective," *American Journal of Physics*, vol. 78, no. 11, pp. 1199-1202, 2010.

[9] S. Savasta, et al., "Nanopolaritons: Vacuum Rabi splitting with a single quantum dot in the center of a dimer nanoantenna," *ACS Nano*, vol. 4, no. 11, pp. 6369-6376, 2010.

[10] C. Wu, et al., "Fano-resonant asymmetric metamaterials for ultrasensitive spectroscopy and identification of molecular monolayers," *Nature Materials*, vol. 11, pp. 69-75, January 2012.

[11] B. Luk'yanchuk, et al., "The Fano resonance in plasmonic nanostructures and metamaterials," *Nature Materials*, vol. 9, pp. 707-715, 2010.

[12] A. B. Khanikaev, C. Wu, and G. Shvets, "Fano-resonant metamaterials and their applications," *Nanophotonics*, vol. 2, no. 4, pp. 247-264, 2013.

[13] R. Adato, S. Aksu, and H. Altug, "Engineering mid-infrared nanoantennas for surface enhanced infrared absorption spectroscopy," *Materials Today*, vol. 00, no. 00, pp. 1-11, March 2015.

[14] C. L. Garrido Alzar, M. A. G. Martinez, and P. Nussenzveig, "Classical analog of electro-megnetically induced transparency," *American Journal of Physics*, vol. 70, no. 1, pp. 37-41, 2002.

[15] X. Zhang, et al., "Electromagnetically induced absorption in a three-resonator metasurface system," *Scientific Reports*, vol. 5, no. 10737, pp. 1-9, May 2015.

[16] W. Wan, W. Zheng, Y. Chen, and Z. Liu, "From Fano-like interference to superscattering with a single metallic nanodisk," *Nanoscale*, vol. 6, no. 15, pp. 9093-9102, May 2014.

[17] A. Lovera, B. Gallinet, P. Nordlander, and O. J. F. Martin, "Mechanisms of Fano resonances in coupled plasmonic systems," *ACS Nano*, vol. 7, no. 5, pp. 4527-4536, April 2013.

[18] S. Zanotto, et al., "Perfect energy-feeding into strongly coupled systems and interferometric control of polariton absorption," *Nature Physics*, vol. 10, no. 11, pp. 830-834, August 2014.

[19] J. Ginn, et al., "Characterizing infrared frequency selective surfaces on dispersive media," *ACES Journal*, vol. 22, no. 1, pp. 184-188, March 2007.

[20] T. Chen, S. Li, and H. Sun, "Metamaterials application in sensing," *Sensors*, vol. 12, no. 3, pp. 2742-2765, February 2012.

[21] D. J. Shelton, et al., "Strong coupling between nanoscale metamaterials and phonos," *Nano Letters*, vol. 11, no. 5, pp. 2101-2108, April 2011.